

# Spontaneous Smith-Purcell radiation described through induced surface currents

J. H. Brownell and J. Walsh

*Department of Physics and Astronomy, Dartmouth College, Hanover, New Hampshire 03755-3528*

G. Doucas

*Particle and Nuclear Physics Laboratory, University of Oxford, Oxford OX1 3RH, United Kingdom*

(Received 6 June 1997; revised manuscript received 19 September 1997)

An analytic solution for the radiated intensity distribution produced by an electron beam passing over a metallic diffraction grating (the Smith-Purcell effect) is derived. The approach is based upon an expression for the current traveling over the grating surface and the method can deal with arbitrary grating profiles. Although collective behavior in the electron beam is neglected, very high power density is predicted if high energy, short electron bunches are employed. The electron beam characteristics of various accelerators are used to illustrate the potential of high energy, accelerator based Smith-Purcell radiation sources. [S1063-651X(98)06201-1]

PACS number(s): 41.60.-m, 42.25.Fx, 42.79.Dj, 41.75.Ht

## I. INTRODUCTION

Since its first observation in 1953 [1], the Smith-Purcell (SP) effect, radiation by electrons passing over a periodic surface, has attracted interest as a source of intense light at otherwise inaccessible wavelengths and as a mechanism for electron acceleration. Many authors have reported SP radiation from the millimeter to visible spectrum [1–12]. Many authors have also developed various theories to characterize the emission process [1,2,13–16]. An accurate yet accessible model has been elusive and the most effective methods to date are general theories of diffraction of light by a grating that can be applied to the SP case, as represented by the van den Berg theory [15].

In the van den Berg theory, incident and diffracted fields are expanded in terms of the independent modes of the metallic grating system and the boundary conditions are matched at the surface. In principle, an arbitrary tooth profile can be analyzed with this approach. In practice, extensive numerical computation is generally required to approach the asymptotic value for the radiation intensity, although there are particular cases that can be solved relatively quickly. Convergence of the numerical solution is particularly difficult to achieve in the regime where the wavelength is small relative to the period [17]. In addition, theories derived from the Helmholtz Green's function (such as the van den Berg model) suffer from an inherent flaw: The Green's function has an infinite set of parametric singularities that renders the theory invalid in the vicinity of the "Rayleigh wavelengths" associated with Wood's anomalies [18].

In the surface current model, presented here, an electron bunch travels parallel to a periodic array of infinitely conductive planar facets. Each facet scatters a continuous frequency spectrum as an electron passes. For a long array, these outgoing waves interfere so that only discrete frequencies are radiated in a given direction. An analytic expression for the approximate radiated intensity is derived that is more physically intuitive and simpler to compute than in the modal expansion theories. Collective electron behavior, and so feedback and stimulated emission, is neglected, but the co-

herent enhancement from a short electron bunch can be included.

## II. RADIATED ENERGY

Assume that the electrons travel at constant velocity  $\mathbf{v} \equiv v\hat{\mathbf{z}}$  parallel to the grating surface and perpendicular to the ruling axis  $\hat{\mathbf{y}}$ . Each electron induces an image charge on the grating surface that keeps pace with it. Variation in the surface causes this induced current to accelerate. From Jackson [19], the energy radiated in the far field per unit frequency per unit solid angle due to a current density  $\mathbf{J}_{\text{total}}$  is

$$W \equiv \frac{\partial^2 I}{\partial \omega \partial \Omega} = \frac{\omega^2}{4\pi^2 c^3} \left| \int dt \int d^3x \hat{\mathbf{n}} \times \hat{\mathbf{n}} \times \mathbf{J}_{\text{total}}(\mathbf{r}, t) e^{i(\omega t - \mathbf{k} \cdot \mathbf{r})} \right|^2,$$

where  $\hat{\mathbf{n}} = \{\hat{\mathbf{x}} \sin \theta \cos \phi + \hat{\mathbf{y}} \sin \theta \sin \phi + \hat{\mathbf{z}} \cos \theta\}$  is the direction of emission,  $\mathbf{k} = \hat{\mathbf{n}} \omega / c$ ,  $\omega$  is the frequency, and  $c$  is the speed of light. (See diagram in Fig. 1.) Since the electron bunch acceleration, a second order effect, is neglected, the bunch itself does not produce a radiating field. The emission is a result of the superluminal space harmonic components in the induced current. Given that the grating is periodic, with period  $\ell$ , over its length  $L$ , the radiating current density can be expressed as the sum of the currents in each tooth:

$$\mathbf{J}_{\text{total}}(\mathbf{r}, t) = \sum_{m=1}^{L/\ell} \mathbf{J}_{\text{tooth}}(\mathbf{r} - m\ell \hat{\mathbf{z}}, t - m\ell/v).$$

Combining these two equations and transforming to coordinates local to a given tooth ( $\mathbf{r} - m\ell \hat{\mathbf{z}} \rightarrow \mathbf{r}$  and  $t - m\ell/v \rightarrow t$ ) yields

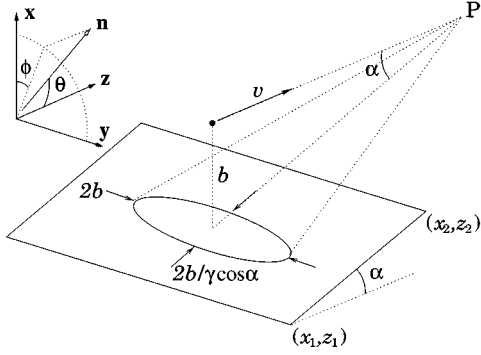


FIG. 1. The oval represents the image charge footprint induced on a single facet by one electron traveling with velocity  $\mathbf{v} = v\hat{\mathbf{z}}$  an instantaneous vertical distance  $b$  above the surface. The point  $P$  is the instantaneous intersection of the electron trajectory and the facet plane. The facet extends infinitely in the  $\hat{\mathbf{y}}$  direction. The emission angles  $\theta$  and  $\phi$  are also shown.

$$W = \frac{\omega^2}{4\pi^2 c^3} \left| \sum_{m=1}^{L/\ell} e^{im\ell\omega(1/v - \hat{\mathbf{n}} \cdot \hat{\mathbf{z}}/c)} \right|^2 \left| \int dt \int d^3x \hat{\mathbf{n}} \times \hat{\mathbf{n}} \times \mathbf{J}_{\text{tooth}}(\mathbf{r}, t) e^{i(\omega t - \mathbf{k} \cdot \mathbf{r})} \right|^2. \quad (1)$$

The sum over the tooth index produces the interference pattern typical of a periodic structure:

$$\left| \sum_{m=1}^{L/\ell} e^{im\ell\omega(1/v - \hat{\mathbf{n}} \cdot \hat{\mathbf{z}}/c)} \right|^2 = \frac{\sin^2[(1/\beta - \cos\theta)\omega L/2c]}{\sin^2[(1/\beta - \cos\theta)\omega \ell/2c]} \rightarrow \sum_{m \neq 0}^{L \gg \ell} \frac{\omega L}{|m|\ell} \delta(\omega - \omega_m). \quad (2)$$

For a grating with a large number of teeth, the emission wavelength is limited to the so-called Smith-Purcell condition,

$$\omega_m \equiv \frac{2\pi|m|c}{\ell(1/\beta - \cos\theta)},$$

where  $m$  is the harmonic mode and  $\beta = v/c$ .

### III. EXPRESSION FOR THE SURFACE CURRENT

The problem, of course, is to find an integrable expression for the current. Consider a tooth profile comprised of  $F$  planar facets where the  $f$ th facet extends from  $\{x_{1f}, z_{1f}\}$  to  $\{x_{2f}, z_{2f}\}$  and to  $y = \pm\infty$ , perpendicular to the  $x$ - $z$  plane. The periodicity of the grating implies that  $z_{2F} - z_{11} \leq \ell$ . Assume that the electron passes, at a height  $x_0$ , either above ( $x_{1f}, x_{2f} \leq x_0$ ) or below ( $x_{1f}, x_{2f} \geq x_0$ ) each facet. Also, let  $z_{1f} \leq z_{2f} \leq z_{1, f+1}$  to avoid inverted and covered facets. Define the angle of inclination of each facet relative to the electron velocity as  $\alpha_f \equiv \tan^{-1}[(x_{2f} - x_{1f})/(z_{2f} - z_{1f})]$ . The image current density within a single tooth then becomes

$$\mathbf{J}_{\text{tooth}}(\mathbf{r}, t) = \sum_{f=1}^F \rho(\mathbf{r}, t, s_f) \mathbf{V}(\mathbf{r}, t, s_f), \quad (3)$$

where  $\rho$  and  $\mathbf{V}$  are the image charge density and velocity and  $s_f$  represents the set  $\{x_{1f}, z_{1f}, x_{2f}, z_{2f}\}$ . This model is applicable to the typical profile of contiguous facets ( $x_{1, f+1} = x_{2f}, x_{2F} = x_{11}, z_{1, f+1} = z_{2f}$  and  $z_{2F} - z_{11} = \ell$ ) as well as cases where the facets are distinct, such as the strip grating and transition radiation. A diagram of a facet orientation is given in Fig. 1.

In the following approximation, the total image charge is a linear superposition of the images due to each electron separately. Therefore, the single electron case shall be derived first. Let the image charge on each facet equal that for an infinite conducting planar surface. This approximation, justified later, neglects the influence of the facet edges on the image charge distribution as well as the image charge due to reflections from other facets. One relativistic electron moving with  $\mathbf{v} = v\hat{\mathbf{z}}$  past an infinite conducting plane defined by  $(x - x_1) = (z - z_1)\tan\alpha$  induces a charge proportional to the component normal to the surface of the electric field produced by an electron in vacuo,

$$\rho(\mathbf{r}, \mathbf{r}_0, t, s) = -\frac{q\gamma}{2\pi} \frac{|(x - x_0)\cos\alpha - (z - z_0 - vt)\sin\alpha|}{[(x - x_0)^2 + (y - y_0)^2 + \gamma^2(z - z_0 - vt)^2]^{3/2}} \delta[(z - z_1)\sin\alpha - (x - x_1)\cos\alpha], \quad (4)$$

where  $q$  is the electron charge,  $\mathbf{r}_0 = (x_0, y_0, z_0)$  is its position at  $t=0$ , and  $\gamma = (1 - \beta^2)^{-1/2}$ . The image charge velocity can be derived by considering that (1) the image would condense to a point at the intersection of the electron trajectory and the facet plane at time  $t' = [z_1 - z_0 + (x_0 - x_1)\cot\alpha]/v$  and (2) since the electric field lines from a solitary electron are radial, the charge distribution scales with the distance of the electron from the surface. The velocity of each image element is then the distance to the intersecting point divided by the transit time:

$$\mathbf{V}(\mathbf{r}, \mathbf{r}_0, t, s) = \frac{\hat{\mathbf{x}}(x_0 - x) + \hat{\mathbf{y}}(y_0 - y) + \hat{\mathbf{z}}(z_0 + vt' - z)}{(t' - t)}.$$

Applying this approximate expression for single electron current to Eq. (1),

$$W_1 \rightarrow \sum_{m \neq 0}^{L \gg \ell} \frac{\omega^3 L}{4\pi^2 |m| c^3 \ell} \delta(\omega - \omega_m) \left| \hat{\mathbf{n}} \times \hat{\mathbf{n}} \times \sum_{f=1}^F \mathbf{j}(\omega, \hat{\mathbf{n}}, \mathbf{r}_0, s_f) \right|^2, \quad (5)$$

where

$$\begin{aligned} \mathbf{j}(\omega, \hat{\mathbf{n}}, \mathbf{r}_0, s) &\equiv \int_{-\infty}^{\infty} dt \int_{z_1}^{z_2} dz \int_{-\infty}^{\infty} dy \int_{-\infty}^{\infty} dx \rho(\mathbf{r}, \mathbf{r}_0, t, s) \mathbf{V}(\mathbf{r}, \mathbf{r}_0, t, s) e^{i(\omega t - \mathbf{k} \cdot \mathbf{r})} \\ &= -\frac{q\gamma}{2\pi} \int_{z_1}^{z_2} dz \int_{-\infty}^{\infty} d\bar{y} \int_{-\infty}^{\infty} du \frac{(\hat{\mathbf{x}}\tan\alpha + \hat{\mathbf{z}})d \pm \hat{\mathbf{y}}\bar{y}\tan\alpha}{[d^2 + \bar{y}^2 + \gamma^2 u^2]^{3/2}} e^{i[\omega(u-z_0)/v + k_y(\bar{y}-y_0) + \kappa z]} e^{-ik_x(x_1 - z_1)\tan\alpha} \end{aligned} \quad (6)$$

and  $u \equiv vt - z + z_0$ ,  $\bar{y} \equiv y_0 - y$ ,  $d \equiv |x_1 - x_0 + (z - z_1)\tan\alpha|$ , and  $\kappa \equiv \omega/v - k_z - k_x \tan\alpha$ . Note that the transit time has canceled out of Eq. (6). Choose the upper sign in Eqs. (6), (7), (8), and (9) if the electron is above the facet ( $x_1, x_2 \leq x_0$ ) or the lower if it is below ( $x_1, x_2 \geq x_0$ ).

Utilizing Ref. [20], Eq. (6) can be reduced to

$$\mathbf{j}(\omega, \hat{\mathbf{n}}, \mathbf{r}_0, s) = -q\ell e^{\mp x_0/2\lambda_e} e^{-i(k_y y_0 + \omega z_0/v)} \mathbf{G}(\omega, \hat{\mathbf{n}}, s), \quad (7)$$

where the evanescent field length is defined as

$$\lambda_e \equiv \left( \frac{2\omega}{\gamma\beta c} \sqrt{1 + \gamma^2 \beta^2 \sin^2 \theta} \right)^{-1}$$

and

$$\begin{aligned} \mathbf{G}(\omega, \hat{\mathbf{n}}, s) &\equiv (\hat{\mathbf{x}}\tan\alpha \pm \hat{\mathbf{y}}i2k_y\lambda_e\tan\alpha + \hat{\mathbf{z}}) \\ &\times \frac{e^{(\pm 1/2\lambda_e - ik_x)(x_1 - z_1)\tan\alpha}}{(\pm \tan\alpha/2\lambda_e + ik_x)\ell} e^{(\pm \tan\alpha/2\lambda_e + ik_x)z} \Big|_{z_1}^{z_2} \end{aligned} \quad (8)$$

is independent of the electron initial position. The particular case of a vertical facet ( $\cos\alpha=0$ ) can be calculated by integrating over  $x$  first, yielding

$$\begin{aligned} \mathbf{G}(\omega, \hat{\mathbf{n}}, x_1, z_1, x_2, z_1) &= (\hat{\mathbf{x}} \pm \hat{\mathbf{y}}i2k_y\lambda_e) \\ &\times \frac{e^{i(\omega/v - k_z)z_1}}{(\pm 1/2\lambda_e - ik_x)\ell} e^{(\pm 1/2\lambda_e - ik_x)x} \Big|_{x_1}^{x_2}. \end{aligned} \quad (9)$$

For the typical configuration where electrons pass *above* the grating (i.e., all facets are below), the energy produced by a single electron then becomes

$$\begin{aligned} W_1 &\xrightarrow{L \gg \ell} \sum_{m \neq 0} \frac{q^2 \omega^3 L \ell}{4\pi^2 |m| c^3} e^{-x_0/\lambda_e} \delta(\omega - \omega_m) \\ &\times \left| \hat{\mathbf{n}} \times \hat{\mathbf{n}} \times \sum_{f=1}^F \mathbf{G}(\omega, \hat{\mathbf{n}}, s_f) \right|^2. \end{aligned} \quad (10)$$

#### IV. SPECIAL CASES

Many special cases have been investigated by earlier workers. One is the strip grating in which thin, coplanar, conducting strips of width  $d$  are aligned such that gaps of width  $\ell - d$  separate them. Using  $F=1$ ,  $x_1 = x_2 = 0$ ,  $z_1 = 0$  and  $z_2 = d$ , integrating Eq. (10) over frequency yields

$$\begin{aligned} \left. \frac{\partial I_1}{\partial \Omega} \right|_{\text{strip}} &\xrightarrow{L \gg \ell} \sum_{m \neq 0} \frac{2}{\pi} \left( \frac{q}{\ell} \right)^2 L (1/\beta - \cos\theta)^{-3} \\ &\times e^{-|x_0|/\lambda_e} \sin^2(\pi m d/\ell) \sin^2 \theta \end{aligned} \quad (11)$$

in agreement with the result derived in approximate form in Ref. [16]. Note that there is no emission for  $d = \ell$ , as expected for a continuous planar surface. In another case, the electron produces transition radiation while passing through slots in a periodic array of thin conducting sheets aligned perpendicular to the electron trajectory. Applying the surface current model to this configuration agrees with the result given in Eq. (1) in Ref. [21].

#### V. COHERENCE

Now consider the case of a bunch of  $N$  electrons, each traveling with velocity  $\mathbf{v} = v\hat{\mathbf{z}}$  *above* a grating. Neglecting collective effects, the derivation proceeds as in the one electron case except that the current, Eq. (3), includes a sum over electrons. The electron initial position-dependent term in Eq. (7), and consequently the sum over electrons, factors out of the sum over facets in Eq. (10), which simplifies the total energy to

$$\begin{aligned} W_N &= W_1 \Big|_{x_0=0} \left| \sum_{a=1}^N e^{-x_a/2\lambda_e} e^{-i(k_y y_a + \omega t_a)} \right|^2 \\ &= W_1 \Big|_{x_0=0} [N S_{\text{inc}} + N^2 S_{\text{coh}}], \end{aligned}$$

where  $(x_a, y_a, z_a)$  is the position of the  $a$ th electron at  $t = 0$ ,  $t_a \equiv z_a/v$ , and the incoherent and coherent sums are

$$S_{\text{inc}} \equiv \frac{1}{N} \sum_{a=1}^N e^{-x_a/\lambda_e},$$

$$S_{\text{coh}} \equiv \frac{1}{N^2} \sum_{a=1}^N \sum_{b \neq a}^N e^{-(x_b + x_a)/2\lambda_e} e^{-i[k_y(y_a - y_b) + \omega(t_a - t_b)]}.$$

Note that these sums should include only those electrons that pass above the top of the grating,  $h = \max(x_{1f}, x_{2f})$ . For large  $N$ , the sums can be replaced by integrals over the distribution in  $x$ ,  $y$ , and  $t$ . Given that the electron positions are uncorrelated, the distribution function factors into three independent functions of each dimension,  $X$ ,  $Y$ , and  $T$  [22]:

$$S_{\text{inc}} \xrightarrow{N \gg 1} \int_h^\infty dx X(x) e^{-x/\lambda_e},$$

TABLE I. Operating parameters of some existing and future accelerators.  $D = \gamma\beta d^2/\epsilon_n$  is the characteristic length of the beam and  $\lambda = 4\pi d/2\gamma\beta$  is the observed wavelength given efficient coupling ( $d = 2\lambda_e$ ). The length  $D$  is the length over which the diameter remains within twice its minimum value  $d$  and therefore is roughly the maximum grating length over which the electron coupling remains efficient.

Facility	Energy (MeV)	$\epsilon_n$ ( $\pi$ mm mrad)	Beam size ( $d$ ) (mm)	Bunch length (mm/ps)	Peak current (A)	$D$ (cm)	$\lambda$ ( $\mu$ m)
Duke [24]	1.2	3.5	$\sim 0.5$	0.3/1	20	7.1	1900
TU-Munich [25]	3	5	$\sim 0.2$	3000/10 <sup>4</sup>	0.5	1.8	182
CIRFEL [26]	14	20	$\sim 0.7$	3.0/10	200	22	157
SUNSHINE [27]	16		$\sim 1.0$	0.2/0.6	48		196
S-DALINAC [28]	38	2	$\sim 0.1$	1.2/4	1.5	12	8
BNL-ATF [29]	50	1	$\sim 0.05$	0.6/2	50	7.9	3
TTF [30]	1000	2	0.055	0.05/0.17	2500	94	0.19

$$S_{\text{coh}} \xrightarrow{N \gg 1} \left| \int_h^\infty dx X(x) e^{-x/2\lambda_e} \tilde{Y}(k_y) \tilde{T}(\omega) \right|^2,$$

where  $\tilde{f}$  is the Fourier transform of  $f$ . When the bunch size is on the order of or less than the wavelength,  $S_{\text{coh}}$  approaches  $S_{\text{inc}}$  and the radiation becomes coherent.

## VI. JUSTIFICATION FOR THE SURFACE CURRENT MODEL

The approximate image charge distribution can be justified as follows. The actual image charge distribution deviates significantly from Eq. (4) only within one distribution half-width of the facet edge. Given that  $b$  is the height of the electron above the grating surface, the distribution half-width in the beam direction is  $\sigma = b/\gamma$ . Neglect of edge effects introduces a relative error in the transform Eq. (6) on the order of the fractional width  $\sigma/\ell$ . The electron couples effectively with the grating if it passes within an evanescent field length. Therefore, under practical conditions when  $b \leq \lambda_e$ , the half-width is limited to

$$\frac{\sigma}{\ell} \leq \frac{1 - \beta \cos \theta}{4\pi|m|}.$$

For low electron energies ( $\beta \ll 1$ ), the half-width is at most 10% of the period. For high energies ( $\beta \approx 1$ ), the emission is focused in the forward direction so that  $\sigma/\ell$  is greatly reduced from the low energy limit. The approximation improves with increasing electron energy.

A preliminary comparison of the results of the surface current and the van den Berg models has been conducted for various echelle gratings over an energy range from 0.1 to 50 MeV. The models agreed well, apart from an overall factor of order one, when a sufficient number of modes were included in the van den Berg calculation. This condition could be satisfied for low energy ( $< 5$  MeV) but, at higher energies, it proved difficult to attain convergence in the van den Berg result and the two methods diverged. Also, the surface current model yields a smooth radiated energy distribution function without the spurious structure around the ‘‘Rayleigh wavelengths’’ generated by the van den Berg model [18].

Two exceptions should be noted. First, since light cannot propagate through bulk metal, the valid angular range of Eq. (10) is limited by the angles of inclination of the facets. Second, in deep tooth profiles several facets may form a cavity and limit the field modes when the wavelength is comparable to or longer than the cavity dimensions. The model described here is best suited for shallow gratings where cavity behavior is negligible but can be applied to deep profiles if the energy is sufficiently high so that the wavelength is much smaller than any cavity.

## VII. RESULTS APPLIED TO VARIOUS ACCELERATORS

The surface current model agrees very well with recent measurements at 3.6 MeV [23]. It is interesting to apply the predictions of our theory to electron beams at other laboratories that are doing, or are planning to do, FEL work. Table I lists the pertinent electron beam parameters for these facilities. Gratings have been installed in the Munich and BNL-ATF facilities but we know of no plans to do so in any of the others listed. Although the table has been compiled from published data on these machines, not all the details were available to us; we could have also misinterpreted some of the numbers. The beam size over the grating, which is a crucial parameter for the effective coupling of the beam to the surface, has in some cases been deduced from the emittance. It is a number that is not inconsistent with the emittance but not necessarily the correct one.

For simplicity, consider experiments involving echelle gratings. To design a grating to match given bunch parameters, the period and blaze angle are adjusted so that the desired wavelength is emitted within the doppler shifted radiation lobe. The peak emitted energy per unit solid angle per electron bunch is not sensitive to the period, as long as the blaze is adjusted accordingly. Since the wavelength is proportional to the period, even a high energy electron beam can produce radiation over a fairly broad spectral range by employing gratings with different periods. Figure 2 displays the spontaneous first order SP energy per unit solid angle per unit grating length per electron bunch achievable at the listed facilities. In each case, the spectral range was chosen arbitrarily and the grating profile then optimized. The bunch temporal profile was assumed to be an inverted parabola:  $J(t) = J_0(1 - t^2/\tau^2)$  within  $-\tau < t < \tau$  and zero otherwise. The peak power, that is, the energy divided by the bunch

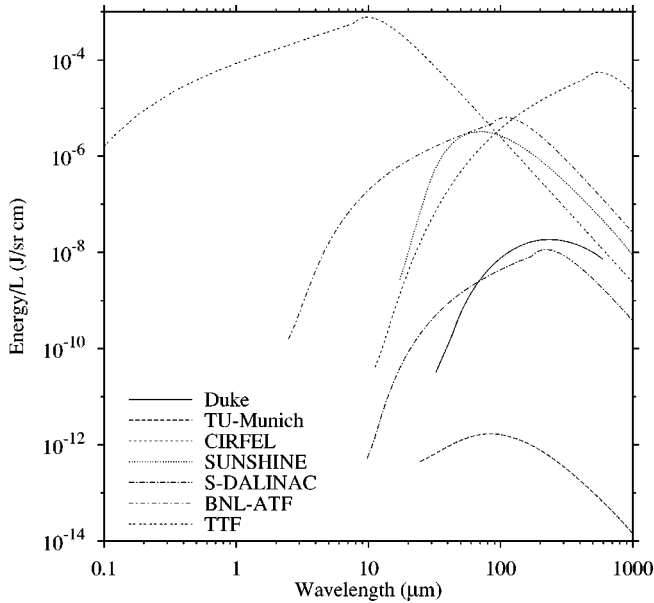


FIG. 2. First order SP energy per unit solid angle per unit grating length per electron bunch produced by echelle gratings given the electron bunch parameters listed in Table I. The grating period and blaze angle are optimized for each facility. The bunch temporal profile was assumed to be parabolic:  $J(t) = J_0(1 - t^2/\tau^2)$  within  $-\tau < t < \tau$  and zero otherwise. For clarity, only the envelope of the interference structure exhibited by parabolic pulses is shown.

length, is shown in Fig. 3. Evidently, the SP process can produce significant amounts of energy and power.

The degree of coherent enhancement is sensitive to the bunch temporal profile. Figure 4 shows the first order SP energy from the BNL-ATF facility due to various temporal profiles when all other bunch and grating parameters are fixed. In order to compare different profiles, the pulse widths are normalized so that half of the electrons arrive within the

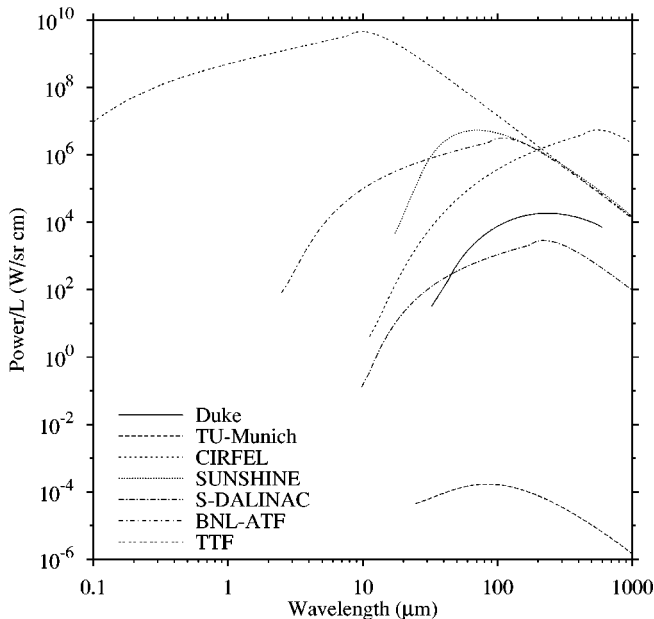


FIG. 3. Peak power: the results in Fig. 2 divided by the bunch length.

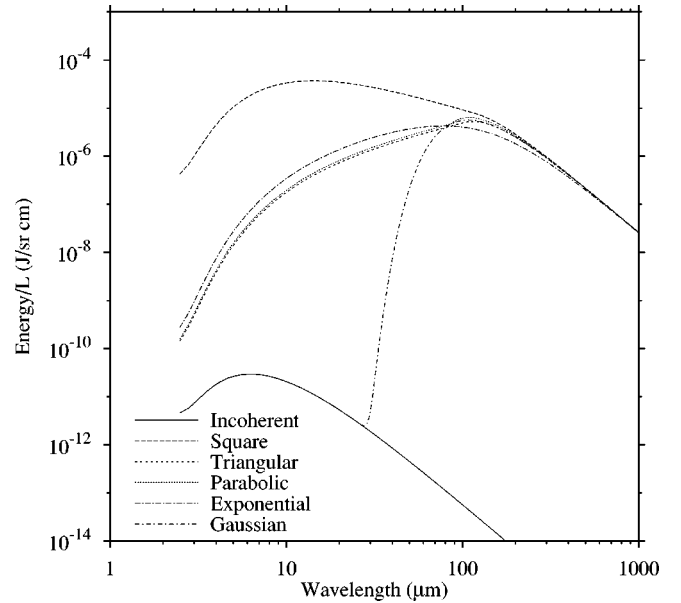


FIG. 4. First order SP energy per unit solid angle per unit grating length per electron bunch produced by a 1 mm period,  $5^\circ$  blaze, echelle grating at the BNL-ATF facility. Five temporal profiles are shown: Square, triangular ( $1 - |t|/\tau$ ), parabolic ( $1 - t^2/\tau^2$ ), exponential [ $\exp(-|t|/\tau)$ ], and Gaussian. For clarity, only the envelope of the interference structure exhibited by square, triangular, and parabolic pulses is shown. All bunch and grating parameters are fixed except that, in order to compare different profiles, the pulse widths ( $\tau$ ) are normalized so that half of the electrons arrive within the nominal bunch length of 2 ps. The solid line indicates the level of purely incoherent radiation ( $S_{\text{coh}} = 0$ ).

nominal bunch length of 2 ps. The square profile has the broadest spectrum and so produces the greatest enhancement at short wavelengths. Likewise, the Gaussian profile produces the least. Triangular, parabolic, and exponential pulses yield similar intermediate values. The solid line indicates the level of purely incoherent radiation. Clearly, with a few billion electrons per pulse, the effect of coherent enhancement is dramatic. The power density that is available in the short electron bunch limit and the ability to choose the center wavelength of the emission suggest many potential applications.

## VIII. CONCLUSION

In conclusion, an analytic description of Smith-Purcell radiation from a metallic grating was derived using an approximate form of the surface current. The surface current model is generally applicable to shallow gratings over a broad electron beam energy range. It is particularly effective when the image charge footprint (itself proportional to the wavelength) is small compared the period. This theory is complementary to modal theories in that the latter are difficult to apply in the short wavelength regime due to the large number of modes involved. The former does not, however, exhibit the spurious behavior near ‘‘Rayleigh wavelengths’’ inherent in the latter. This model also has the benefits of very short computation time and simple physical interpretation of the result, both of which facilitate grating design.

## ACKNOWLEDGMENTS

We would like to acknowledge the support of the U. S. Army Research Office Grant No. DAAH04-95-1-0640 and helpful comments by C. Platt and J. Urata. The authors are

also pleased to acknowledge the hospitality of Dr. Ilan Ben-Zvi and his ATF staff, and extended technical discussions with Dr. R. Fernow and Dr. H. Kirk from Brookhaven National Laboratory.

- 
- [1] S. J. Smith and E. M. Purcell, *Phys. Rev.* **92**, 1069 (1953).  
 [2] W. W. Salisbury, *Science* **154**, 386 (1966).  
 [3] J. P. Bachheimer, *Phys. Rev. B* **6**, 2985 (1972).  
 [4] E. L. Burdette and G. Hughes, *Phys. Rev. A* **14**, 1766 (1976).  
 [5] A. Gover, P. Dvorkis, and U. Elisha, *J. Opt. Soc. Am. B* **1**, 723 (1984).  
 [6] I. Shih, W. W. Salisbury, D. L. Masters, and D. B. Chang, *J. Opt. Soc. Am. B* **7**, 345 (1990).  
 [7] I. Shih *et al.*, *J. Opt. Soc. Am. B* **7**, 351 (1990).  
 [8] I. Shih *et al.*, *Opt. Lett.* **15**, 559 (1990).  
 [9] G. Doucas *et al.*, *Phys. Rev. Lett.* **69**, 1761 (1992).  
 [10] K. J. Woods *et al.*, *Phys. Rev. Lett.* **74**, 3808 (1995).  
 [11] M. Goldstein *et al.* (unpublished).  
 [12] K. Ishi *et al.*, *Phys. Rev. E* **51**, R5212 (1995).  
 [13] G. Toraldo di Francia, *Nuovo Cimento* **16**, 61 (1960).  
 [14] K. Ishiguro and T. Tako, *Opt. Acta* **8**, 25 (1961).  
 [15] P. M. van den Berg, *J. Opt. Soc. Am.* **63**, 1588 (1973).  
 [16] J. Walsh, K. Woods, and S. Yeager, *Nucl. Instrum. Methods Phys. Res. A* **341**, 277 (1994).  
 [17] O. Haerberlé, P. Rullhusen, J.-M. Salomé, and N. Maene, *Phys. Rev. E* **49**, 3340 (1994).  
 [18] J. F. Bird, *Opt. Commun.* **136**, 349 (1997).  
 [19] J. D. Jackson, *Classical Electrodynamics*, 2nd ed. (John Wiley & Sons, Inc., New York, 1975).  
 [20] I. Gradshteyn and I. Ryzhik, *Table of Integrals, Series, and Products* (Academic Press, San Diego, 1980), eqs. 3.771.2 and 6.726.3-4.  
 [21] M. J. Moran, *Phys. Rev. Lett.* **69**, 2523 (1992).  
 [22] J. S. Nodvick and D. S. Saxon, *Phys. Rev.* **96**, 180 (1954).  
 [23] J. H. Brownell, G. Doucas, and J. Walsh, *J. Phys. D* **30**, 2478 (1997).  
 [24] S. V. Benson, J. M. Dutta, C. R. Jones, H. Kosai, in *Micro Bunches Workshop*, edited by E. B. Blum, M. Dienes, and J. B. Murphy, AIP Conf. Proc. No. 367 (AIP, New York, 1995), p. 350.  
 [25] T. Kormann, G. Korschinek, C. Stan-Sion, M. Dumitru, G. Doucas, and M. F. Kimmitt, in *Proceedings of the 5th European Particle Accelerator Conference (EPAC96)*, edited by S. Myers, A. Pacheco, R. Pascual, Ch. Petit-Jean-Genaz, and J. Poole (IOP, Bristol, (1996), Vol. 1, p. 748.  
 [26] I. Lehrman *et al.*, *Nucl. Instrum. Methods Phys. Res. A* **341**, 31 (1994).  
 [27] D. Bocek, P. Kung, H. C. Lihn, C. Settakorn, and H. Wiedemann, SLAC report SLAC-PUB-95-6985.  
 [28] A. Richter, in *Proceedings of the 5th European Particle Accelerator Conference (EPAC96)* (Ref. [25]), Vol. 1, p. 110.  
 [29] X. J. Wang, X. Qiu, and I. Ben-Zvi, *Phys. Rev. E* **54**, R3121 (1996).  
 [30] R. Corsini and A. Hofmann, in *Proceedings of the 5th European Particle Accelerator Conference (EPAC96)* (Ref. [25]), Vol. 1, p. 721.